Effect of Single-Side Modulation Doping on Low-Temperature Transport Properties in Square Infinite Quantum Wells

Nguyen Huyen Tung[1], Doan Nhat Quang[2] and Do Thi Hien[2]

[1] Institute of Engineering Physics, HUT, 1 Dai Co Viet Road, Hanoi, Vietnam
[2] Centre for Theoretical Physics, VAST, 10 Dao Tan Str., Hanoi, Vietnam

Abstract. A variational approach is given for the effect from single-side modulation doping on low-temperature transport properties of the charge carriers confined in a square infinite quantum well (QW). We obtained analytic expressions which describe the doping effects on the carrier distribution in the well, their roughness-induced scattering in the in-plane and screening by them. The calculation of the transport lifetimes is performed for holes in a SiGe/Ge/SiGe square QW, and the result is found in quantitative agreement with recently measured dependence on experimental conditions such as channel width and carrier density.

1. Introduction

Modulation doped strained Ge and SiGe-based quantum wells (QWs) have received enormous attention in recent years due to their importance in device applications. In order to upgrade the hole mobility of the above-quoted QWs, one needs to identify the key scattering mechanisms limiting the transport properties of their two-dimensional hole gas (2DHG), and reduce their detrimental effects. It is well known [1,2] that the best way for this purpose is to study the dependence of 2DHG mobility on experimental conditions such as sample temperature, carrier density, and channel width.

It is worth to mention that although the above dependencies were explored by a number of authors, they still remain as challenging problems. Firstly, there are several reports [3–5] on the channel width dependence of the 2DHG mobility measured in a strained Ge channel in $Si_{1-x}Ge_x/Ge/Si_{1-x}Ge_x$ QWs. This exhibits a pronounced peak, which is in sharp contrast to the monotonic increase predicted by the normally adopted theories [6], but, to date no theoretical analysis available. Secondly, the key scattering mechanisms for these QWs are a subject under debate. The previous interpretations of some experimental findings are quite different even due to one and the same research group [4,8]. Indeed, from the 2DHG mobility dependence on temperature (≤ 100K) and on channel width some authors [3,4,8] assumed surface roughness scattering to be the key mechanism. However, from the carrier density dependence of the mobility and the transport to quantum lifetime ratio, the others [8] assumed ionized impurity scattering to be dominant. Thirdly, in their calculations the roughness-related misfit deformation potential scattering has been ignored, which was proven to be important for

strained Si [10] and SiGe [11] channels. Just recently, some experimental [8] and theoretical [12] studies have indicated that the doping-induced confinement may be of great importance for the QW mobility. To date, the theory of doping effect on quantum confinement has been developed for triangular QWs [9], however, no theory for square QWs available. Thus, the goal of this paper is to provide a theory of the band-bending effect on the low-temperature transport properties of charge carriers in a single-side modulation doped infinite square QW. We develop a variational approach to the description of quantum confinement in bent-band infinite square QWs.

2. Single-Side Modulation Doped Infinite Square QW

2.1 Variational Wave Function for a Single-Side Modulation Doped Infinite Square QW

As a prototype, we are dealing with a heterostructure made of cubic crystals, which is composed of a strained well layer grown pseudomorphically along the [001] axis between two barrier ones. The well layer forms a conduction channel of width L in the region $|z|<L/2$. The sample is modulation doped in a region of thickness L_d in the surface-side barrier $z<-L/2$ and separated from the channel by a spacer layer of thickness L_s. The confinement may be plausibly described by an asymmetric wave function as follows:

$$\zeta(z)=\begin{cases} Bk^{1/2}(\cos kz)e^{-k'z} & for\ \ |z|<L/2 \\ 0 \quad for\ \ |z|>L/2, \end{cases} \tag{1}$$

in which B, k, and k' are variational parameters to be determined; k and k' are wave numbers in the well layer with k' quantifying the doping – induced band bending effect. The boundary conditions at the interface planes and the normalization read as follows:

$$k=\pi/L,\ \ \pi B^2\gamma_1(c)/2=1, \tag{2}$$

where $c=k'L$, and $\gamma_1(c)$ is in Eq.(A3), so c is the single independent variational parameter. In the absence of doping $c = 0$, this goes to the exact symmetric wave function of an ideally-square well (flat-band model) [6]. Thus, the parameter c quantifies the effect of the doping-induced band bending on the wave function.

2.2 Hartree Potential in a Single-Side Modulation Doped Infinite Square QW

The wave function of the lowest subband is obtained by minimizing the total energy per particle which is determined by the Hamiltonian

$$H=T+V_H(z), \tag{3}$$

where T is the kinetic energy, and $V_H(z)$ is the Hartree potential as a confining potential along the growth direction. The latter is created by the ionized remote impurities and charge carriers in the well in accordance with Poisson's equation

$$\frac{d^2}{dz^2}V_H(z) = \frac{4\pi e^2}{\varepsilon_L}\left[N_I(z) - p(z)\right], \tag{4}$$

in which $N_I(z)$ is the bulk density of impurities (per unit volume), $p(z)$ the one of carriers, and ε_L is the dielectric constant of the QW. The sample is modulation doped with an impurity density N_I in a region in the top barrier from $-z_d$ to $-z_s$, where the doping positions: $z_d = L_d + L_s + L/2$ and $z_s = L_s + L/2$, so that

$$N_I(z) = \begin{cases} N_I, & \text{for } -z_d \le z \le -z_s \\ 0, & \text{elsewhere.} \end{cases} \quad \text{and} \quad p(z) = p_s\left|\zeta(z)\right|^2 \tag{5}$$

with p_s as a sheet carrier density. We solve Poisson's equation (4) in combination with electrostatic boundary conditions, especially the vanishing of the relevant electric field at infinity $z \to \pm\infty$. As a result, within the variational approximation with the use of the wave function from Eq. (1), the Hartree potential may be separated into two parts:

$$V_H(z) = V_I(z) + V_s(z)\,. \tag{6}$$

The first term V_I from Eq. (6) is to be regarded as the impurity potential fixed by the doping profile, viz. the impurity density N_I and doping positions z_d, z_s; while the second one V_s as the 2DHG potential fixed by the sheet hole density p_s and their distribution, i.e., the variational parameters.

2.3 Total Energy Per Particle in the Lowest Subband

We now turn to the total energy per particle in the ground-state subband. The expectation value for the Hamiltonian from Eqs. (3) and (6) is a function of the bending parameter c, given by

$$E(c) = \langle T\rangle + \langle V_I\rangle + \langle V_s\rangle\,. \tag{7}$$

The total energy per particle is given by Eq. (7), in which the average potential due to the carrier distribution is to be replaced by its half. For the kinetic energy, it holds

$$\langle T\rangle = \frac{-\hbar^2}{2m_z L^2}\frac{\pi B^2}{2}\left[\left(c^2 - \pi^2\right)\gamma_1(c) + 2\pi c\,\omega_1(c)\right], \tag{8}$$

where m_z is the out-of-plane carrier effective mass of the well material, γ_n and ω_n with n as an integer are simple functions of a variable defined by Eqs. (A3) and

(A4). Next, the average potential due to charged impurities can be written in terms of the dimensionless doping positions: $d = z_d/L$ and $s = z_s/L$, as

$$\langle V_I \rangle = \frac{4pe^2}{e_L}\frac{N_I L^2}{2}\left(d^2 - s^2\right). \tag{9}$$

Lastly, for the carrier potential it holds

$$\begin{aligned}\langle V_s \rangle = \frac{4\pi e^2}{\varepsilon_L}\frac{p_s L}{4}\Bigg\{ & \pi B^2\left[\left(2\frac{g_-}{L} + g'_-\right)\gamma_1(c) - g' + \frac{\partial\gamma_1(c)}{\partial c}\right] \\ & -\frac{\pi^2 B^4}{4}\gamma_1(2c)\left[\frac{1}{c^2} + \frac{c^2-\pi^2}{\left(c^2+\pi^2\right)^2} + \frac{c^2-\pi^2}{2\left(c^2+\pi^2\right)^2}\left[\gamma_2(2c) - \gamma_0(2c)\right]\right] \\ & +\frac{\pi^2 B^4}{4}\left[\frac{\pi c}{\left(c^2+\pi^2\right)^2}\left[\omega_2(2c) + 2\omega_1(2c)\right]\right]\Bigg\}.\end{aligned} \tag{10}$$

3. Low-Temperature Transport Lifetime

3.1 Basic Equations

In this section we are dealing with transport properties of charge carriers confined in a single-side modulation doped infinite square QW, viz., their transport lifetime τ_t.

The particles moving along the in-plane are scattered by various disorder sources which are characterized by some random fields. Scattering by a Gaussian random field is specified by its autocorrelation function in wave vector space $\langle |U(\mathbf{q})|^2 \rangle$. Here $U(\mathbf{q})$ is a two-dimensional Fourier transform of the unscreened scattering potential weighted with an envelope wave function

$$U(\mathbf{q}) = \int_{-\infty}^{+\infty} dz \left|\zeta(z)\right|^2 U(\mathbf{q}, z). \tag{11}$$

At very low temperature the charge carriers are in general expected to experience the following scattering mechanisms: (i) remote impurities (RI), (ii) surface roughness (SR) from both interfaces, and (iii) misfit deformation potential (DP) therefrom. The overall lifetime is determined by the ones for individual disorders according to the Matthiessen's rule

$$\frac{1}{\tau_{tot}} = \frac{1}{\tau_{RI}} + \frac{1}{\tau_{SR}^{(t)}} + \frac{1}{\tau_{SR}^{(b)}} + \frac{1}{\tau_{DP}^{(t)}} + \frac{1}{\tau_{DP}^{(b)}}, \tag{12}$$

with the superindex (t) referring to the top interface and (b) to the bottom one**,** respectively. Within the linear transport theory, the inverse transport lifetime for zero temperature is represented in terms of the autocorrelation function for each disorder by [6]

$$\frac{1}{\tau_t}=\frac{1}{(2\pi)^2\hbar E_{\mathrm{F}}}\int_0^{2k_F}dq\int_0^{2\pi}d\varphi\frac{q^2}{\left(4k_F^2-q^2\right)^{1/2}}\frac{\langle|U(\mathbf{q})|^2\rangle}{\varepsilon^2(q)}, \tag{13}$$

here $\mathbf{q}(q,\varphi)$ denotes the 2D momentum transfer by a scattering event in the (x-y) plane (in polar coordinates), $q = |\mathbf{q}| = 2k_F\sin(\theta/2)$ with θ as a scattering angle. The Fermi energy is given by $E_F = \hbar^2k_F^2/2m^*$, with k_F as the Fermi wave number fixed by the sheet carrier density: $k_F = (2\pi p_s)^{1/2}$, and m^* as the in-plane carrier effective mass of the well. The dielectric function $\varepsilon(q)$ entering Eq. (13) takes account of the screening of a scattering potential by charge carriers. As usual, this is evaluated within the random phase approximation

$$\varepsilon(q)=1+\frac{q_s}{q}F_S(q)\left[1-q/2\left(q^2+k_F^2\right)^{1/2}\right],\quad \text{for } q\le 2k_F \tag{14}$$

with $q_s = 2m^*e^2/\varepsilon_L\hbar^2$ as the inverse 2D Thomas-Fermi screening length. The screening form factor $F_S(q)$ takes account of the extension of particle states along the growth direction, defined by

$$F_S(q)=\int_{-\infty}^{+\infty}dz\int_{-\infty}^{+\infty}dz'\left|\zeta(z)\right|^2\left|\zeta(z')\right|^2e^{-q|z-z'|}. \tag{15}$$

The calculation of the screening form factor with the wave function given by Eq. (1) is lengthy. As a result, one may achieve an analytic expression:

$$F_S(t)=\left(\pi^2B^4/4\right)[S^{(u)}(t)+S^{(l)}(t)], \tag{16}$$

with $t = qL$ as the dimensionless in-plane wave number. The functions figuring here are defined as follows:

$$\begin{aligned}S^{(u/l)}(t)=&\pm\frac{1}{2(c\mp t/2)}\left[e^{\pm(c\mp t/2)}\gamma_1(c\pm t/2)-\gamma_1(2c)\right]\\&\pm\frac{\pi}{4[\pi^2+(c\mp t/2)^2]}[\,\omega_2(2c)+2\omega_1(2c)]\\&\mp\frac{c\mp t/2}{4[\pi^2+(c\mp t/2)^2]}\left[2e^{\pm(c\mp t/2)}\gamma_1(c\pm t/2)+\gamma_2(2c)+2\gamma_1(2c)-\gamma_0(2c)\right],\end{aligned} \tag{17}$$

where the upper (lower) signs refer to the subindex (u) and (l), respectively.

In the doping-free condition ($c = 0$), the above expression is simplified to the one for the flat-band model [6].

3.2 Autocorrelation Functions for Scattering Mechanisms

Remote impurity

As known, [6,13] the autocorrelation function for scattering from a random distribution of charged impurities is supplied by an integral over the doping region:

$$\langle | U_{RI}(q) |^2 \rangle = \left(\frac{2\pi e^2}{\varepsilon_L q} \right)^2 \int_{-\infty}^{+\infty} dz_i N_I(z_i) F_R^2(q, z_i), \tag{18}$$

where $N_I(z_i)$ is the three-dimensional impurity density given by Eq. (5). $F_R(q,z_i)$ denotes the form factor for a sheet of impurities in the plane z_i defined by

$$F_R(q, z_i) = \int_{-\infty}^{+\infty} dz \, |\zeta(z)|^2 \, e^{-q|z-z_i|} . \tag{19}$$

The calculation of Eq. (19) with the wave function from Eq. (1) yields

$$F_R(q, z_i) = \pi B^2 \frac{e^{qz_i}}{2} \gamma_1(c + qL/2) . \tag{20}$$

However, the sample is usually subjected to thermal treatment during epitaxial growth. Therefore, one has to take into account the Coulomb repulsion between charged impurities during their diffusion, which weakens their averaged field.

Accordingly, the high-temperature ionic correlation is proven to diminish their autocorrelation function by some factor $t/(t+t_c)$, where

$$t_c = (2\pi e^2 n_I L)/(\varepsilon_L k_B T_0) , \tag{21}$$

with n_I as the sheet impurity density: $n_I = (N_I)^{2/3}$, T_0 as the freezing temperature for impurity diffusion, and k_B the Boltzmann constant. Consequently, we may arrive at the following autocorrelation function for remote impurities:

$$\left\langle \left| U_{RI}(t) \right|^2 \right\rangle_c = \frac{N_I L^3}{4} \left(\frac{2\pi e^2}{\varepsilon_L} \right)^2 \frac{\pi B^2 \gamma_1(c + t/2)}{2} \frac{e^{-2st} - e^{-2dt}}{t^2 (t + t_c)} , \tag{20}$$

where $\langle \ldots \rangle_c$ stands for the averaging over correlated impurities.

Surface roughness

We now turn to scattering related to interface roughness, viz., surface roughness and misfit deformation potential. The former is an event which arises from

roughness-induced fluctuations in position of the potential barriers. The weighted scattering potential in wave vector space is determined by the value of the wave function at the interface planes $\varsigma_{\pm} = \varsigma(z = \pm L/2)$ [13]:

$$U_{SR}(q) = V_0 \left|\zeta_{\pm}\right|^2 \Delta_{\mathbf{q}}, \tag{21}$$

where $\Delta_{\mathbf{q}}$ denotes a Fourier transform of the interface profile. The scattering rate calculated with the use of a variational wave function might be much larger than the one calculated numerically self-consistently. For getting rid of this problem we need to establish a formula for the weighted roughness potential in terms of such quantities that are insensitive to the trial wave function, e.g., its large peak and some integral quantities on the z axis. For the wave function from Eq. (1), this peak is located at a point $z_0 = \delta L$, with $\delta = -(1/\pi)\arctan(c/\pi)$ and $|\delta| < 1/2$.

For the above set purpose, we integrate the one-dimensional Schrodinger's equation with the Hamiltonian fixed by Eqs. (3) along the growth direction from $z = 0$ to $z = \pm\infty$. With some wave function $\varsigma(z)$ we may arrive at the following relations:

$$V_0 \left|\zeta_{-}\right|^2 = \left[E(c) - V_H(z_0)\right] \zeta^2(z_0) + \int_{-\infty}^{z_0} dz\, \zeta^2(z) \frac{\partial V_H(z)}{\partial z}, \tag{22}$$

$$V_0 \left|\zeta_{+}\right|^2 = \left[E(c) - V_H(z_0)\right] \zeta^2(z_0) - \int_{z_0}^{+\infty} dz\, \zeta^2(z) \frac{\partial V_H(z)}{\partial z}, \tag{23}$$

where $E(c)$ is the particle energy given by Eq. (7). From Eqs. (22) and (23), it holds for scattering from the top and bottom rough interfaces that

$$V_0 \zeta_{\mp}^2 = \left[E(c) - V_H(z_0)\right] \zeta^2(z_0) \pm \frac{4\pi e^2}{\varepsilon_L} \frac{p_s}{8} W^{(t/b)}, \tag{24}$$

where by definition:

$$\begin{aligned} W^{(t/b)} = {} & 4\pi B^2 g'_{+} \Gamma_1(\pm c; \pm\delta) + \pi^2 B^4 \left\{ \left[\frac{1}{c} + \frac{c}{c^2 + \pi^2} \right] \Gamma_1(\pm 2c; \pm\delta) \right. \\ & + \frac{c}{2(c^2 + \pi^2)} \left[\Gamma_2(\pm 2c; \pm\delta) - \Gamma_0(\pm 2c; \pm\delta \right] \\ & \left. \mp \frac{\pi}{2(c^2 + \pi^2)} \left[\Omega_2(\pm 2c; \pm\delta) + 2\Omega_1(\pm 2c; \pm\delta \right] \right\}, \end{aligned} \tag{25}$$

with Γ_n and Ω_n as simple functions of two variables defined by Eqs. (A1) and (A2). The upper signs on the right-hand side of Eq. (25) refer to the top interface (t), and the lower signs to the bottom one (b). It follows from Eq. (21) that the

surface roughness scattering depends strongly on the interface profile. This is normally written as follows:

$$\langle |\Delta_q|^2 \rangle = \pi \Delta^2 \Lambda^2 F_{SR}(t), \tag{26}$$

where Δ is a roughness amplitude, and Λ is a correlation length. The form factor for surface roughness is well described by a form of Gaussian type distribution:

$$F_{SR}(t) = \exp(-t^2 \Lambda^2 / 4L^2). \tag{27}$$

Misfit deformation potential

In the pseudomorphic QW under study the well layer is assumed to be under strain. The in-plane component of the strain field in the well is fixed by a lattice mismatch as follows:

$$\in_{\|} = (a_{\|} - a_0)/a_0, \tag{28}$$

where $a_{\|}$ and a_0 are the lattice constants of this layer in the presence and in the absence of strain. It has been demonstrated [6,10] that interface roughness produces fluctuations in the strain field. These strain fluctuations in turn induce nonuniform shifts of the band edges, and so act on the charge carriers as a scattering source. It should be stressed that the misfit deformation potentials for two kinds of carrier are quite different, viz., the one for electrons is fixed by a single normal diagonal component of the strain field [6], whereas the one for holes by all its components [11].

The roughness-induced misfit deformation potential for holes in a cubic crystal is

$$U_{DP}^{(t/b)}(q,z) = \frac{\alpha \in_{\|}}{2} q \Delta_q e^{\mp(z \pm L/2)} \times \left\{ \frac{3}{2}\left[b_s(K+1)\right]^2 (1+\sin^4\varphi+\cos^4\varphi) + \left(\frac{d_s G}{4c_{44}}\right)^2 (1+\sin^2\varphi\cos^2\varphi) \right\}^{1/2} \tag{29}$$

in the well ($|z| \leq L/2$) and zero elsewhere. Here the upper and lower signs again refer to the top (t) and bottom (b) interfaces, respectively. In Eq. (29) b_s and d_s are the shear deformation potential constants of the well layer, and its anisotropy ratio is α, elastic constants K, G are given in [11].

Upon averaging this potential with the wave function from Eq. (1), we may obtain the autocorrelation function of interest in an analytic form:

$$\left\langle \left| U_{DP}^{(t/b)}(q) \right|^2 \right\rangle = \left(\frac{\pi^{3/2} \alpha \in_{\parallel} \Delta\Lambda}{4} \right)^2 \left(\frac{B^2}{L} \right)^2 \left[\frac{3}{2} \left[b_s (K+1) \right]^2 (1 + \sin^4 \varphi + \cos^4 \varphi) + \left(\frac{d_s G}{4 c_{44}} \right)^2 (1 + \sin^2 \varphi \cos^2 \varphi) \right] F_{DP}^{(t/b)}(t) \,, \tag{30}$$

where the form factor is defined by

$$F_{DP}^{(t/b)}(t) = t^2 e^{-t} \gamma_1^2 (c \pm t/2) F_{SR}(t) \,, \tag{31}$$

with $t = qL$ and $F_{SR}(t)$ from Eq. (27).

4. Results and Conclutions

4.1 Validity of the Model and Input Parameters

In what follows, we will use the theory developed above to study the low-temperature transport properties of single-side modulation doped infinite square QWs. As an example, the theory is illustrated for the 2DHG in a $Si_{1-x}Ge_x/Ge/Si_{1-x}Ge_x$ QWs sample, where the Ge channel is under in-plane biaxial compressive strain. We will show how to explain the recent experimental data about the dependence on channel width [3–5], and on carrier density [7, 9] of the 2DHG mobility. Thereby, we are able to identify the key scattering mechanisms for holes in the Ge channel of this heterostructure.

We now outline a discussion of the validity of the assumptions adopted in the formulation. As pointed out in [14] for strained Ge on cubic $Si_{1-x}Ge_x$ with Ge content $x \bigcirc 0.7$ the potential barrier height is somewhat large: $V_0 \leftrightarrow 300$ meV. Thus, for not narrow Ge channels ($L \leftrightarrow 50$), the infinite square QW model may be acceptable as in earlier theories [9,11]. Thus, for not wide Ge channels ($L \bigcirc 160$) and not high carrier densities ($p_s \bigcirc 2 \times 10^{12}$ cm^{-2}), the single-subband scattering model may be acceptable.

For numerical calculation, we used the lattice constants, elastic stiffness constants, dielectric constants, and shear deformation potentials listed in [15] for Si and Ge. The corresponding constants for a $Si_{1-x}Ge_x$ alloy are estimated within the virtual crystal approximation. For strained Ge the

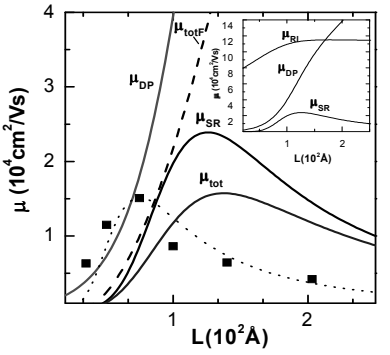

Fig. 1. Partial and total mobilities μ of holes in a $Si_{0.33}Ge_{0.67}/Ge/Si_{0.33}Ge_{0.67}$ square QW vs chanel width L. The 20K experimental data [4] are marked by squares. The dotted line is total mobiliy of the bent-band model with $p_s = 5.10^{12}$cm^{-2}

out of-plane hole effective mass is fixed m_z=0.19m_e, while the in-plane hole effective mass is supplied by measurement in [7] as an increasing function of carrier density owing to nonparabolicity of the valence band.

4.2 Numerical Results and Comparison with Experiment

To end this section, we attempt to explain some recent experimental findings about the 2DHG mobility in square Ge QWs. We first deal with the channel width dependence of the mobility for the sample studied in [4], made of $Si_{0.33}Ge_{0.67}$/ $Ge/Si_{0.33}Ge_{0.67}$ with a lattice mismatch $\varepsilon_{\|}$ = –0.01. The sample was modulation doped with a thickness L_d = 100, a spacer L_s = 200. The partial and overall mobilities limited by the above scatterings are plotted at a hole density p_s = 1x10^{12} cm^{-2} versus channel width L in Fig. 1, where the measured 20K data [4] is represented for a comparison.

Next, we are concerned with the carrier density dependence of the transport in the sample studied in [7], made of $Si_{0.3}Ge_{0.7}/Ge/Si_{0.3}Ge_{0.7}$. The doping is the same as in Fig. 1, but with a smaller spacer L_s = 100. The partial and overall mobilities limited by the diverse scatterings are plotted at a channel width L = 75 versus hole density p_s in Fig. 2, where the measured 8K data [7] is also represented.

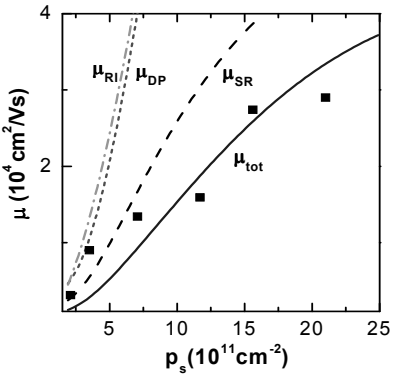

Fig. 2. Partial and total mobilities μ of holes in a $Si_{0.33}Ge_{0.67}/Ge/Si_{0.33}Ge_{0.67}$ square QW with a chanel width L = 75 vs hole density p_s. The 8K experimental data [7] are marked by squares

From the lines thus obtained, we may draw the following conclusions:
(i) As clearly observed from Fig. 1, the calculated overall mobility may reproduce very well the observed channel width dependence of the 2DHG mobility. The key scattering mechanisms are surface roughness and misfit deformation potential, remote impurities are in general less relevant.
(ii) The channel width evolution shows up in a pronounced mobility maximum for a channel of $L_{max} \sim 130$ nearly equal to the one specified by experiment [4]. This peak was also detected by other groups [3,5] at somewhat larger L_{max}.

5. Summary

In this report we have provided a theory of the band-banding effect on the transport properties of charge carriers confined a single-side modulation-doped infinite square QW. In contrast to the earlier belief, we have shown that the peak in the channel width evolution of the mobility appears as an effect of the doping-induced band bending.

6. Auxiliary Functions

These are defined as an algebraic combination of elementary functions by

$$\Gamma_n(\eta;\nu) = \frac{e^{\eta} - e^{-2\nu\eta}}{2\eta} + \frac{1}{2(\eta^2 + n^2\pi^2)}[(-1)^n \eta e^{\eta} + e^{-2\nu\eta}(n\pi \sin 2\nu n\pi - \eta \cos 2\nu n\pi)], \tag{A1}$$

$$\Omega_n(\eta;\nu) = \frac{1}{2(\eta^2 + n^2\pi^2)}[(-1)^n n\pi e^{\eta} + e^{-2\nu\eta}(n\pi \cos 2\nu n\pi + \eta \sin 2\nu n\pi)], \tag{A2}$$

$$\gamma_n(\eta) = \left[\frac{1}{\eta} + \frac{(-1)^n \eta}{\eta^2 + n^2\pi^2}\right] \sinh \eta, \tag{A3}$$

$$\omega_n(\eta) = (-1)^n n\pi \frac{\sinh \eta}{\eta^2 + n^2\pi^2}. \tag{A4}$$

References

1. F. Schaffler, *Semiconductor Science and Technology* **12**, 1515 (1997).
2. T. E. Whall and E. H. C. Parker, *Journal of Physics* D **31**, 1397 (1998).
3. Y. H. Xie, D. Monroe, E. A. Fitzgerald, P. J. Silverman, F. A. Thiel, and G. P. Watson, *Applied Physics Letters* **63**, 2263 (1993).
4. T. Irisawa, H. Miura, T. Ueno, Y. Shiraki, *Japanese Journal of Applied Physics* **40**, 2964 (2001).
5. R. J. H. Morris, T. J. Grasby, R. Hammond, M. Myronov, O. A. Mironov, D. R. Leadley, T. E. Whall, E. H. C. Parker, M. T. Currie, C. W. Leitz, and E. A. Fitzgerald, *Semiconductor Science and Technology* **19**, L106 (2004).
6. A. Gold, *Physical. Review*. B **35**, 723 (1987).
7. T. Irisawa, M. Myronov, E. H. C. Parker, K. Nakagawa, M. Murata, S. Koh, and Y. Shiraki, *Applied Physics Letters* **82**, 1425 (2003).
8. M. Myronov, K. Sawano, and Y. Shiraki, *Applied Physics Letters* **88**, 252115 (2006).
9. B. Rossner, D. Chrastina, G. Isella, H. von Kanel, *Applied Physics Letters* **84**, 3058 (2004).
10. R. M. Feenstra and M. A. Lutz, *Journal of Applied Physics* **78**, 6091 (1995).
11. D. N. Quang, N. H. Tung, D. T. Hien, and H. A. Huy, *Physical. Review*. B **75**, 073305 (2007).
12. D. N. Quang, N. H. Tung, V. N. Tuoc, N. V. Minh, H. A. Huy, and D. T. Hien, *Physical. Review*. B **74**, 205312 (2006).
13. T. Ando, A. B. Fowler, and F. Stern, *Reviews of Modern Physics* **54**, 437 (1982).
14. Kahan, M. Chi, and L. Friedman, *Journal of Applied Physics* **75**, 8012 (1994).
15. G. Van de Walle,*Physical. Review*. B **39**, 1871 (1989).

http://www.springer.com/978-3-540-88200-8

Physics and Engineering of New Materials

Cat, D.T.; Pucci, A.; Wandelt, K.R. (Eds.)
2009, XI, 387 p., Hardcover
ISBN: 978-3-540-88200-8